CHEMICAL ENGINEERING TRANSACTIONS
VOL. 92, 2022
A publication of AIDIC
The Italian Association of Chemical Engineering
Online at www.cetjournal.it
Guest Editors: Rubens Maciel Filho, Eliseo Ranzi, Leonardo Tognotti

ISBN 978-88-95608-90-7; **ISSN** 2283-9216
DOI: 10.3303/CET2292057

Biomass in Li-O_2 Batteries? Deep Discharge Performance of an O_2 Electrode Based on Humins

Jean Felipe Leal Silva, Emília Savioli Lopes, Chayene Gonçalves Anchieta, Maria Regina Wolf Maciel, Gustavo Doubek, Rubens Maciel Filho

Advanced Energy Storage Division – Center for Innovation on New Energies (AES/CINE), School of Chemical Engineering, University of Campinas (UNICAMP). Rua Michel Debrun, s/n, Campinas, SP, Brazil, ZIP code 13083-841.
jefelipe@outlook.com; jefelipe@feq.unicamp.br

Humins are a by-product of the hydrolysis of carbohydrates in the production of levulinic acid. With the development of new large-scale processes to produce levulinic acid, the production of large amounts of this by-product will demand new applications beyond burning in biomass furnaces. Owing to its carbonaceous nature, many value-added applications have been considered. One of these applications is in the production of carbon-based electrodes for batteries. Such application has great potential because of the increasing need for the development of new cost-competitive energy storage technologies with enhanced specific energy. In this context, Li-O_2 batteries are a technology with potential specific energy higher than current state-of-the-art lithium-ion batteries. This work reports the synthesis of a humins-based O_2 electrode for a Li-O_2 battery. Humins synthesized as a by-product of hydrolysis of sugars were purified via leaching, dried, and thermally treated under an inert atmosphere to enhance their electronic conductivity. The obtained product was then mixed with a binder and templated over a stainless-steel mesh to obtain the O_2 electrode. Batteries were assembled with electrodes based on humins from both sugarcane bagasse and molasses. Humins were analyzed via X-ray photoelectron spectroscopy and scanning electron microscopy before and after treatments, and the electrodes were analyzed before and after the discharge of the battery. Results of deep discharge demonstrate the potential for this material for the manufacturing of carbon-based electrodes for batteries.

1. Introduction

The development of biorefineries for the use of biomass and renewable resources for the production and replacement of fossil-based products has been shown as an effective strategy for the reduction of emissions of greenhouse gases (Hossain et al., 2017). An important component of the biorefinery approach is to seek value-added applications for all biomass fractions and the by-products of their processing. One of the possible biorefinery layouts is the thermochemical conversion of biomass which can be used to produce levulinic acid and furfural from cellulose and hemicelluloses (Tacchini et al., 2020). This process consists on the hydrolysis of polysaccharides and dehydration of sugars, and these conditions also lead to the production of humins, a by-product of condensation reactions of sugars and furans.

Currently, the main potential application for humins is as a supplementary boiler fuel (Leal Silva et al., 2021a). Nevertheless, other applications as catalyst support have been already proposed because of the low cost of this material and the possible properties of carbon-based materials. In this context, a potential application for this by-product is the production of electrodes for Li-O_2 batteries (Thakkar et al., 2021). Li-O_2 batteries represent one of the next frontiers in the development of electrochemical energy storage devices because of their potentially high specific energy (Leal Silva et al., 2021b). In the development of this battery, several materials have been being tested for the manufacture of the O_2 electrode. This part of the battery must present high surface area, porosity, catalytic activity, and conductivity to act as a suitable support for the deposition of discharge product, which is Li_2O_2 (Tan et al., 2017). Among the possible candidates under consideration by the scientific community, carbon-based materials deserve special attention because of the possibility of fine-tuning many of their properties to make them suitable for this application.

Paper Received: 4 December 2021; Revised: 27 March 2022; Accepted: 3 May 2022
Please cite this article as: Leal Silva J.F., Lopes E.S., Anchieta C.G., Wolf Maciel M.R., Doubek G., Maciel Filho R., 2022, Biomass in Li-o2 Batteries? Deep Discharge Performance of an O2 Electrode Based on Humins, Chemical Engineering Transactions, 92, 337-342 DOI:10.3303/CET2292057

Based on this possible application of a biorefinery residue in the production of an electrochemical energy storage device, this work presents the synthesis and testing of an experimental O_2 electrode for a Li-O_2 battery based on humins from sugarcane bagasse and sugarcane molasses. Humins were synthesized, purified, and thermally annealed. The chemical composition and morphology of samples from each step were analyzed via several methods. Discharge tests of these electrodes demonstrate the potential of this material in the production of electrodes, thus showing a new application for humins produced during the synthesis of levulinic acid from biomass.

2. Methodology

2.1 Synthesis and purification of humins

Humins were synthesized from two sources. Sugarcane bagasse was obtained from Usina São João (Araras, São Paulo, Brazil), and sugarcane molasses was obtained from Usina Ester (Cosmópolis, São Paulo, Brazil). Samples were stored in the freezer without any treatment. Humins from sugarcane bagasse were synthesized by mixing sugarcane bagasse with a 1 w/v% H_2SO_4 aqueous solution with 10% solids loading. The mixture was heated and kept at 170 °C for 75 min (Lopes et al., 2020). The resulting solid fraction (H-SCB) was recovered by filtration for further treatment. Humins from molasses were synthesized by mixing 100 parts of 9 w/v% H_2SO_4 aqueous solution with 123 parts of sugarcane molasses, and the mixture was heated and kept at 160 °C for 80 min (Lopes et al., 2021). The resulting solid fraction (H-SCM) was recovered by filtration for further treatment. Both solid fractions were dried at 80 °C under vacuum for 12 h. Then, Soxhlet extraction with water was performed in 3 cycles of 8 h each, and the solids were dried at 80 °C under vacuum for 12 h.

2.2 Preparation of electrodes

Purified humins were ground using an agate mortar and pestle and then thermally annealed on a horizontal tube furnace (LT3.3010, Jung, Brazil) under argon flow in a two-step process. In the first step, the samples were heated to 375 °C (heating rate of 5 °C min^{-1}) for 2 h and left to cool. Then, the samples were heated to 850 °C (heating rate of 5 °C min^{-1}) for 3 h and left to cool (van Zandvoort et al., 2013). The resulting carbon samples (C-SCB or C-SCM) were ground once again. A slurry consisting of 18 w% treated carbon and 2 w% Nafion (solution, 20.7 w% Nafion™ perfluorinated resin in 34:45 water:1-propanol, Sigma-Aldrich) in isopropanol (>98%, Sigma-Aldrich) was sonicated for 2 minutes in a tip sonicator (Eco-sonics QR 550W, Ultronique, Brazil). The slurry was dropped into previously weighted 16 mm discs of stainless-steel wire mesh (wire diameter: 40 µm, opening size: 50–55 µm) over a Petri dish, which was left to dry for 24 h in an oven at 50 °C. The electrodes were peeled off, weighed, and stored in a desiccator.

The batteries were assembled with a Li foil (Tob Machine, 99.99%), a glass microfiber membrane (GF/A, Whatman), and the O_2 electrode (based on H-SCB or H-SCM) using a solution of 0.1 mol L^{-1} lithium perchlorate ($LiClO_4$, ≥99.99% trace metal basis, Sigma-Aldrich) in dimethylsulfoxide (DMSO, ≥99.9%, Sigma-Aldrich) as the electrolyte whose water content was measured via coulometric Karl Fischer titration (852 Titrando Metrohm AG, Switzerland). Batteries were assembled inside a glovebox workstation (H_2O and O_2<10 ppm, Ar atmosphere, MBraun MB10, M. BRAUN Inertgas-Systeme GmbH) and left to rest for 1 h before testing. After the assembling process, the batteries were filled with pure O_2 at a pressure of 3 bar to initiate the deep discharge test.

2.3 Deep discharge test and analysis of electrodes

After a resting period of 30 min, the battery was discharged at a current of 50 µA using an Arbin Potentiostat/Galvanostat (LBT21084, Arbin Instruments LLC, USA) until the cut-off potential of 2.2 V. Then, the cell was purged with N_2 and disassembled inside the glovebox workstation. The discharge capacity was normalized by the weight of treated carbon deposited onto the stainless-steel template. The morphology of the treated carbon samples of H-SCB and H-SCM and the electrodes after discharge were analyzed using scanning electrode microscopy (SEM, Quattro S, Thermo Fischer Scientific Inc., USA) at a beam energy of 10 kV, and a working distance of 10 mm. The chemical composition of the surface of samples before and after treatment was analyzed using X-ray photoelectron emission spectroscopy (XPS, K-Alpha, Thermo Fischer Scientific Inc., USA) and energy-dispersive X-ray spectroscopy (UltraDry, Thermo Fischer Scientific Inc., USA).

3. Results and Discussion

3.1 Synthesized humins and carbon electrodes

Figure 1 shows pictures of the humins samples after purification and after thermal annealing, and Figure 2 shows SEM micrographs of the humins after purification, after thermal annealing, and after battery discharge. According to these results, it is possible to observe that the mild conditions used in the hydrolysis of sugarcane bagasse produced a sample consisting of unconverted biomass covered with humins. Results from SEM show

that grinding the samples after purification produced powders with an average particle size of 3.9 ± 2.8 µm for H-SCB and 4.0 ± 1.3 µm for H-SCM. After thermal annealing and grinding, particle size was 3.7 ± 2.7 µm for C-SCB and 3.9 ± 1.2 µm for C-SCM. Therefore, thermal annealing did not have any impact on particle size. In the case of C-SCB, the particle size distribution followed a Weibull distribution, with 66% of them smaller than average and some particles as large as ~50 µm. In the case of C-SCM, particle size distribution followed a normal distribution and generally presented a spherical shape of similar size. Many spheres were grouped into clusters of 23 ± 11 µm by sintering, which is a problem because it reduces the surface area of the material.

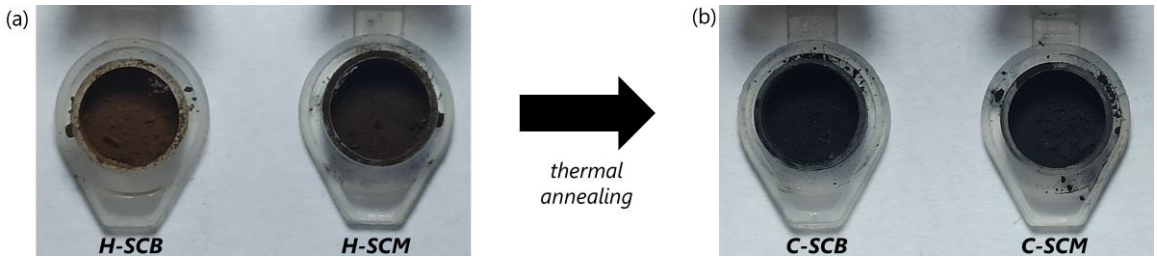

Figure 1: Humins samples (a) after purification (left: H-SCB, right: H-SCM) and (b) after thermal annealing (left: C-SCB, right: C-SCM).

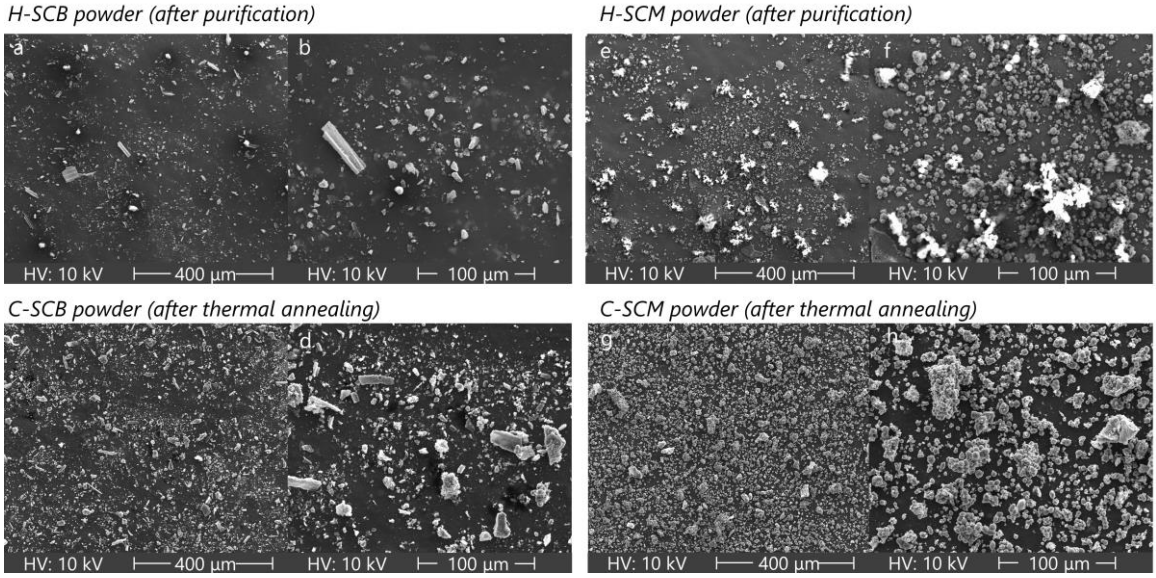

Figure 2: SEM micrographs of samples a, b) H-SCB, c, d) C-SCB, e, f) H-SCM, and g, h) C-SCM in different magnifications using the Everhart–Thornley detector

SEM micrographs in Figure 2 were obtained using integration mode to avoid anomalies because of charging effects in samples with poor electronic conductivity. Micrographs at live and integration modes to compare the electronic conductivity of both materials before and after thermal annealing. According to these analyses, thermal annealing increased the electronic conductivity of both samples, which is a fundamental property in the development of carbon-based electrodes. This process step was more important for the electrode based on sugarcane bagasse because of the very low conductivity observed in this sample before thermal annealing. According to EDS results, thermal annealing increased the C/O atomic ratios from 2.06 to 20.4 in the samples based on sugarcane bagasse and from 1.69 to 24.9 in the sample based on sugarcane molasses. This reduction in the oxygen content greatly increases the conductivity of carbon-based materials (Morimoto et al., 2016). Moreover, the reduction in oxygen content of the samples without the reduction of particle size as discussed before might indicate a porosity increase after thermal annealing. Sulfur was observed to be a contaminant of the samples in trace amounts because of the catalyst employed in hydrolysis (H_2SO_4). XPS analysis of S (not shown here) indicates a higher detection of this element bound to C only in the thermally treated samples in trace amounts.

XPS spectra of carbon for all samples are shown in Figure 3 and indicate the predominance of C-C bonds in all samples. Peak integration also shows the reduction of O after thermal treatment of samples. Based on these results, it is possible to see that thermal annealing reduced the functionalization of carbon. Moreover, a π–π* satellite peak is observed with a binding energy that is 6 eV higher than the main C-C peak, thus indicating the presence of extended delocalized electrons (Morgan, 2021). The presence of these delocalized electrons contributes to the theory that thermal treatment increases the conductivity of humins-derived carbon.

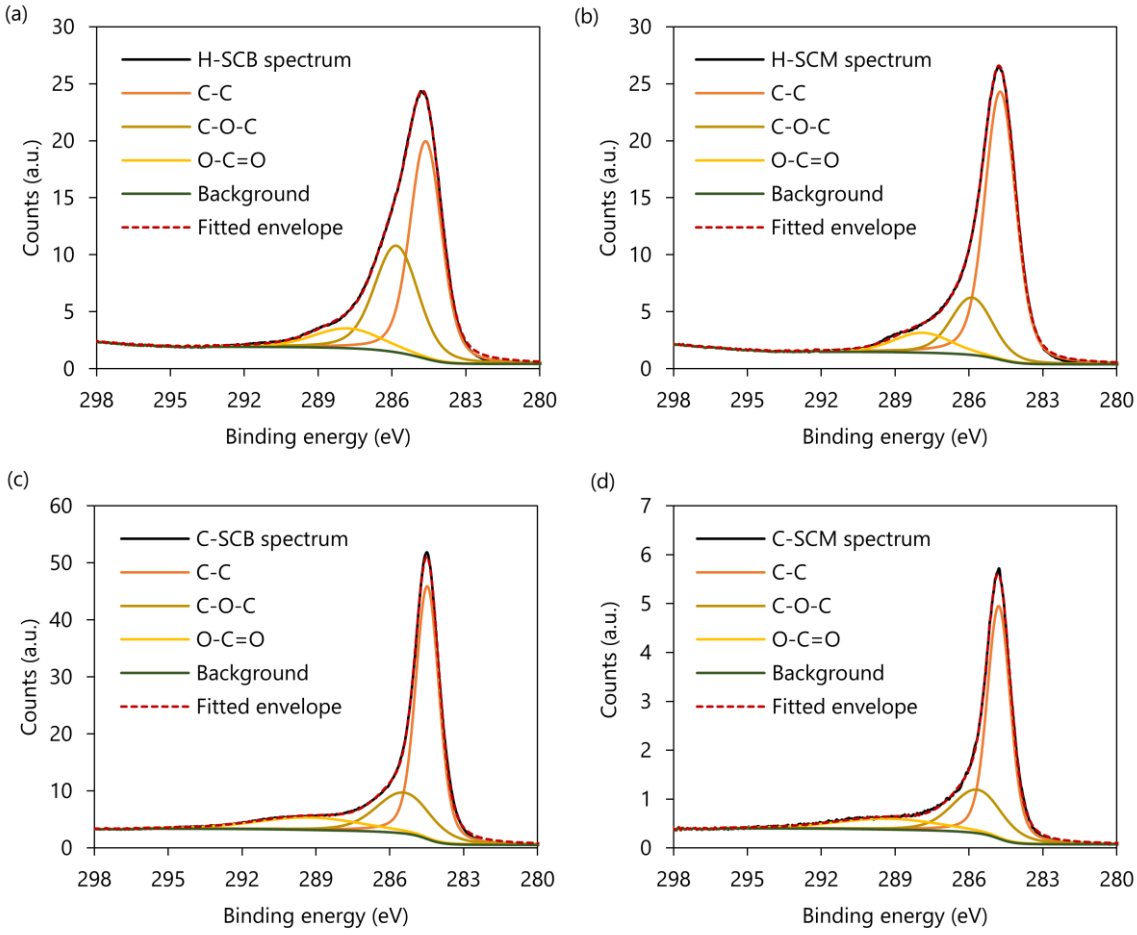

Figure 3: XPS C1s spectra of a) H-SCB, b) H-SCM, c) C-SCB, and d) C-SCM

3.2 Deep discharge tests

Figure 4 shows the deep discharge curves for electrodes based on C-SCB and C-SCM. According to these results, the specific capacity of electrodes based on C-SCM is 51% higher than electrodes based on H-SCB. In both cases, the discharge occurred with a potential plateau mostly above 2.75 V, indicating a low discharge overpotential. However, as the discharge product covered the entire carbon surface (Figure 2), the potential of the cell dropped fast to the cut-off potential of 2.2 V because of the high resistivity of the discharge product (Li_2O_2). This potential drop to the cut-off potential at the end of discharge occurs faster for the electrode based on C-SCM because of the higher uniformity in particle size, as shown in Figure 2.

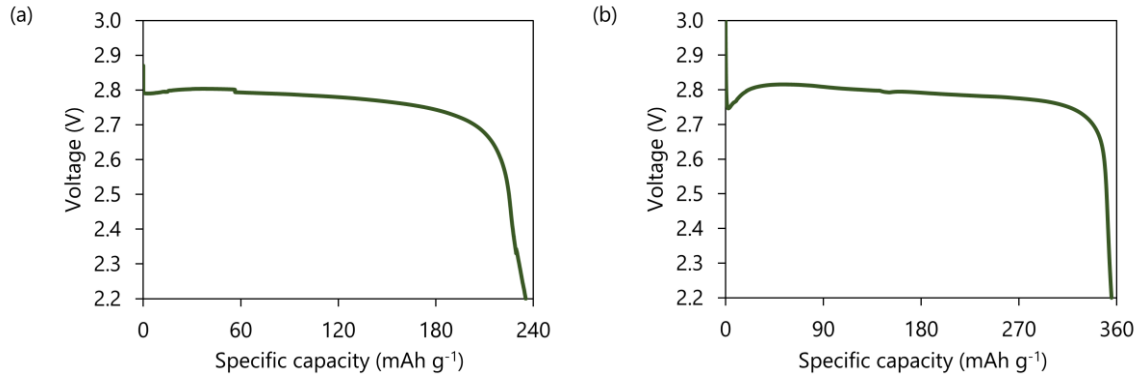

Figure 4: Deep discharge curves for O_2 electrodes based on (a) C-SCB and (b) C-SCM

Figure 5 presents the morphology and distribution of the discharge product in both electrodes. It is possible to observe that the discharge product covered uniformly both electrodes. According to the results of Karl-Fischer titration, the electrolyte contained 97 ppm of water. The morphology of the discharge product observed in Figure 5b and Figure 5f is similar to results previously reported in the literature (Aetukuri et al., 2015) for an electrolyte with low water concentration over a carbon-based electrode. Based on this comparison, discharge tests with electrolytes with more water might lead to increased capacity.

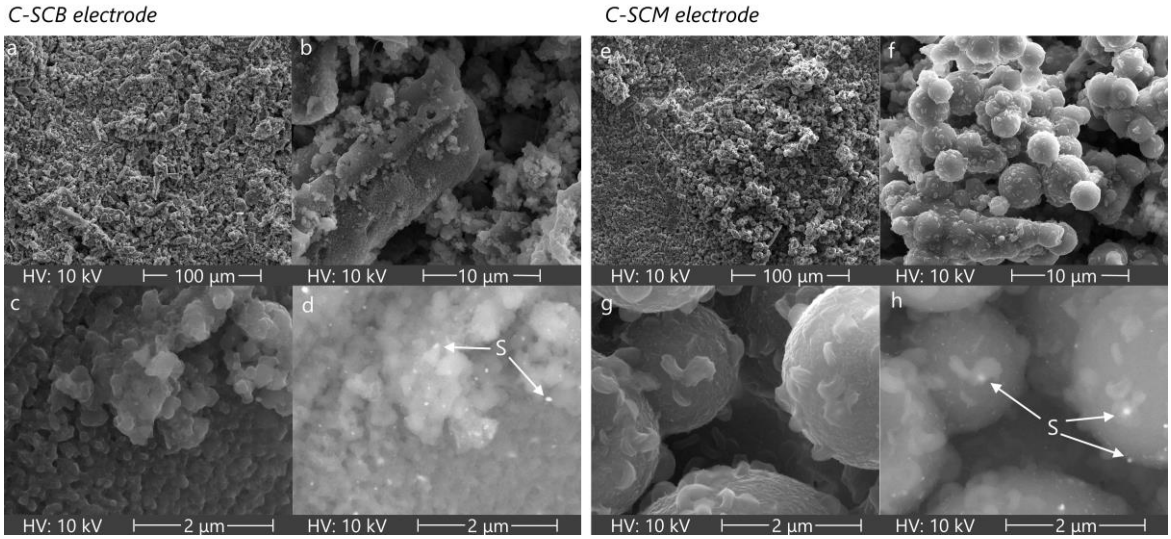

Figure 5: SEM micrographs of electrodes a-d) C-SCB and e-h) C-SCM in different magnifications; images in the bottom show the same area using the Everhart–Thornley (c and g, left) and backscatter (d and h, right) detectors

In the case of the electrode based on C-SCB, the discharge product also covered large particles of unhydrolyzed biomass (Figure 5b). In the case of the electrode based on C-SCM, the spherical particles were evenly covered by the discharge product, with the formation of crystals that resemble the shape of a red blood cell. In the case of smaller agglomerates, more discharge product accumulated over their surface. Another interesting finding is that the particle size of the Li_2O_2 particles forming at the surface is small compared to the size of the humins-based carbon spheres. The use of smaller spheres can increase the available surface area and improve the specific capacity of the material. Therefore, humins obtained in different hydrolysis conditions, with different particle sizes (van Zandvoort et al., 2013), should be tested as well to determine the impact of particle size on the specific capacity of this electrode material. Another point that deserves attention is the presence of sulfur, shown in Figure 5d and Figure 5h, because the impact of trace amounts of this element should be considered as well in the study of the stability of this electrode material.

4. Conclusion

This work presented the first results of discharge tests of O_2 electrodes for Li-O_2 batteries based on sugarcane-derived humins, which is a by-product of the thermochemical conversion of bagasse or molasses to levulinic acid. Results of specific capacity demonstrate the potential of using this material for the manufacturing of O_2 electrodes with low discharge overpotential. Images of the discharge product indicate that adjusting the electrolyte composition and particle size can lead to increased discharge capacity. Results also indicate high functionalization of this material. Additional analyses should be performed on these materials to assess their stability in the potential window that is suitable for most electrolytes of Li-O_2 batteries, and tests should also consider humins obtained in different reaction conditions with possible different particle sizes.

Acknowledgments

The authors gratefully acknowledge the support from FAPESP (the Sao Paulo Research Foundation, Grant Numbers 2015/20630-4, 2016/10450-1, 2017/11958-1, and 2018/16663-2), Shell, the strategic importance of the support given by ANP (Brazil's National Oil, Natural Gas, and Biofuels Agency) through the R&D levy regulation, the Brazilian National Council for Scientific and Technological Development and (CNPq, Grant Number 150313/2020-9), and the Coordenação de Aperfeiçoamento de Pessoal de Nível Superior - Brasil (CAPES) - Finance Code 001.

References

Aetukuri N.B., McCloskey B.D., García J.M., Krupp L.E., Viswanathan V., Luntz A.C., 2015, Solvating Additives Drive Solution-Mediated Electrochemistry and Enhance Toroid Growth in Non-Aqueous Li–O_2 Batteries, Nature Chemistry, 7(1):50–56.

Hossain G.S., Liu L., Du G.C., 2017, Industrial Bioprocesses and the Biorefinery Concept, Current Developments in Biotechnology and Bioengineering: Bioprocesses, Bioreactors and Controls, 3–27.

Leal Silva J.F., Doubek G., Maciel Filho R., 2021b, Impact of the Catalytic Activity of Carbon Nanotubes in the Performance of Li-O_2 Batteries, Chemical Engineering Transactions, 86:499–504.

Leal Silva J.F., Mariano A.P., Maciel Filho R., 2021a, Less Severe Reaction Conditions to Produce Levulinic Acid with Reduced Humins Formation at the Expense of Lower Biomass Conversion: Is It Economically Feasible?, Fuel Communications, 9:100029.

Lopes E.S., Leal Silva J.F., Rivera E.C., Gomes A.P., Lopes M.S., Maciel Filho R., Tovar L.P., 2020, Challenges to Levulinic Acid and Humins Valuation in the Sugarcane Bagasse Biorefinery Concept, Bioenergy Research, 13:757–74.

Lopes E.S., Leal Silva J.F., Nascimento L.A., Bohórquez J.F.C., Lopes M.S., Tovar L.P., Maciel Filho R., 2021, Feasibility of the Conversion of Sugarcane Molasses to Levulinic Acid: Reaction Optimization and Techno-Economic Analysis, Industrial and Engineering Chemistry Research, 60(43):15646–57.Morgan, David J. 2021. "Comments on the XPS Analysis of Carbon Materials, C 2021, Vol. 7, Page 51 7(3):51.

Morimoto N., Kubo T, Nishina Y., 2016, Tailoring the Oxygen Content of Graphite and Reduced Graphene Oxide for Specific Applications, Scientific Reports, 6(1):1–8.

Tacchini E., Moreno V.C., Tugnoli A., Cozzani V., 2020, Technical-Economic Analysis of Processes for the Production of Levulinic Acid, Chemical Engineering Transactions, 80:277–82.

Tan P., Jiang H.R., Zhu X.B., An L., Jung C.Y., Wu M.C., Shi L., Shyy W., Zhao T.S., 2017, Advances and Challenges in Lithium-Air Batteries, Applied Energy, 204:780–806.

Thakkar A., Shell K.M., Bertosin M., Rodene D.D., Amar V., Bertucco A., Gupta R.B., Shende R., Kumar S., 2021, Production of Levulinic Acid and Biocarbon Electrode Material from Corn Stover through an Integrated Biorefinery Process, Fuel Processing Technology, 213:106644.

van Zandvoort I., Wang Y., Rasrendra C.B., van Eck E.R.H., Bruijnincx P.C.A., Heeres H.J., Weckhuysen B.M., 2013, Formation, Molecular Structure, and Morphology of Humins in Biomass Conversion: Influence of Feedstock and Processing Conditions, ChemSusChem, 6(9):1745–58.